# Letters

## Closed-Loop Black Start-Up of Dual-Active-Bridge Converter With Boosted Dynamics and Soft-Switching Operation

Jingxin Hu, *Member, IEEE*, Shenghui Cui, *Member, IEEE*, and Rik W. De Doncker, *Fellow, IEEE*

***Abstract*—This letter proposes a closed-loop black start-up control for the dual-active-bridge (DAB) converter. With a simple combination of the extended phase-shift and triple phase-shift modulation schemes, the DAB converter can start up with the maximum allowable precharge current while realizing soft-switching operation in the trapezoidal current mode simultaneously. Compared to the conventional start-up procedure that usually requires multiple steps of operation and parameter fine-tuning, the proposed start-up method can be implemented simply into the existing closed-loop controller and can shorten the start-up transients of the DAB converter significantly. The presented methods are validated experimentally on a downscaled DAB converter prototype.**

***Index Terms*—Black start-up, closed-loop control, dual active bridge (DAB), inrush current, soft switching.**

### I. Introduction

THE dual active bridge (DAB) is a popular dc–dc converter topology to transfer a bidirectional power flow over a wide voltage range with galvanic isolation and soft-switching operation [1]. Since the DAB converter is widely used as a dc transformer in grid and industrial applications, the black start-up is a crucial function to restore the system after faults or maintenance and enhance the system stability and availability [2].

In the black start-up procedure, the fully discharged output dc capacitor of the DAB converter needs to be precharged from the input side. However, when directly applying the steady-state switching pattern, e.g., the single phase-shift (SPS) modulation [1], a high inrush current occurs in the ac link, which results in excessive thermal stress and potential failures in the power semiconductor devices [3]. To address this issue, soft start-up procedures are proposed in [4]–[6], which first operate the output bridge only as a diode rectifier and increase the inner phase shift of the input bridge gradually in an open-loop manner. When the output dc capacitor is naturally charged to the maximum rectification voltage, the output bridge starts switching, and the closed-loop control is enabled to regulate the output voltage to the final reference value gradually. To ensure a suppressed inrush current in the whole start-up procedure, the aforementioned method requires a careful manual fine-tuning of the parameters under different load conditions [5], [6], i.e., the ramp slope-rate of both the inner phase shift and the reference voltage. This makes such methods less generic and difficult to optimize. Moreover, as the maximum peak value of the inrush current is only limited but not fully utilized in the whole procedure, those multistep approaches have an inherent limitation in the start-up speed. In [3], the dual phase-shift modulation is proposed to reduce the inrush current during start-up, but further analysis and evaluation are still needed. In [7], the extended phase-shift (EPS) modulation is also considered to increase the precharge current at the start-up in an open-loop manner, but the mode selection and parameter calculation are rather complex. Besides, multiple steps of operation are also required in the start-up procedure.

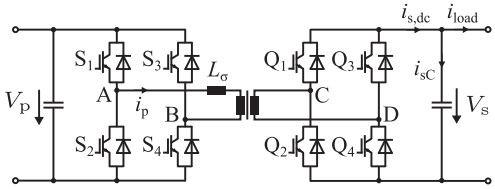


Fig. 1. Circuit diagram of single-phase DAB converter.

In this letter, a dedicated EPS mode is proposed, which is particularly suitable for a low output voltage operation with a high output current. Combined with the triple phase-shift (TPS) modulation [8], the DAB converter can realize a closed-loop start-up control with a fully regulated inrush current, a boosted start-up speed and soft-switching operation.

### II. State-of-the-Art Soft Start-Up Procedure

The single-phase DAB consists of two H-bridges with ac voltages denoted by $v_{\mathrm{AB}}$ and $v_{\mathrm{CD}}$ and a high-frequency transformer with a leakage inductance $L_\sigma$ and a turns ratio $N_{\mathrm{tr}}$, as depicted in Fig. 1. As illustrated in Fig. 2, the state-of-the-art soft start-up procedure is generally divided into two steps.

Manuscript received March 15, 2021; revised April 1, 2021; accepted April 5, 2021. Date of publication April 7, 2021; date of current version June 30, 2021. This work was supported in part by European Union's Horizon 2020 Research and Innovation Programme under Grant 957788 through Project HYPERRIDE, and in part by the Federal Ministry of Education and Research (BMBF, FKZ03SF0490), Flexible Electrical Networks Research Campus. *(Corresponding author: Shenghui Cui.)*

The authors are with the Institute for Power Generation and Storage Systems, E.ON ERC and the FEN Research Campus, RWTH Aachen University, 52062 Aachen, Germany (e-mail: jhu@eonerc.rwth-aachen.de; scui@eonerc.rwth-aachen.de; dedoncker@ieee.org.).

Color versions of one or more figures in this letter are available at https://doi.org/10.1109/TPEL.2021.3071578.

Digital Object Identifier 10.1109/TPEL.2021.3071578

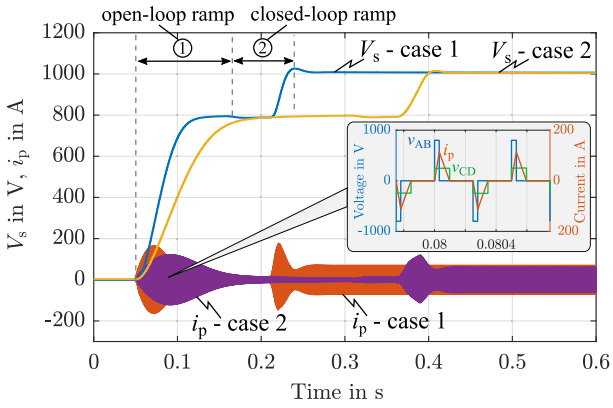


Fig. 2. Key waveforms of the state-of-the-art soft start-up procedure (case 1: high-slope ramp-rate; case 2: low-slope ramp-rate).

The first step is known as the open-loop ramp phase, where only the gate signals of $S_1 - S_4$ in the input bridge are activated. The inner phase-shift ratio of the input H-bridge $D_p$ increases from 0 to 0.5 linearly with a slope ramp-rate $\frac{dD_p}{dt}$. The typical ac voltages and current waveforms are also shown in Fig. 2. The inner phase-shift determines the duty ratio of $v_{AB}$, which limits the peak value of the transformer current when the output voltage is still low. Meanwhile, the resulting triangular transformer current flows into the output diode rectifier and charges the output capacitor until the output voltage $V_s$ reaches the input one $V_p$ (a turns ratio $N_{tr} = 1$ is assumed hereinafter without loss of generality). $\frac{dD_p}{dt}$ is the key design parameter in this stage. As shown in Fig. 2, a lower $\frac{dD_p}{dt}$ in case 2 results in a lower peak inrush current but a longer ramp time of the output dc voltage. However, considering the nonlinear slope of $V_s$ especially when a load is connected, a generic analytical design of $\frac{dD_p}{dt}$ for different load conditions is challenging. This usually leads to a conservative choice of $\frac{dD_p}{dt}$ and a long start-up duration.

The second step, known as the closed-loop ramp phase, starts when $V_s$ is equal or sufficiently close to $V_p$. The gate signals of $Q_1 - Q_4$ in the output bridge are also activated, and the closed-loop voltage control is enabled to regulate $V_s$. If the final reference value $V_s^*$ is different from $V_p$, a ramp slope-rate $\frac{dV_s^*}{dt}$ is also required to limit the peak current, as depicted in Fig. 2, which is also difficult to calculate analytically.

Therefore, the state-of-the-art soft start-up method requires a careful fine-tuning of both $\frac{dD_p}{dt}$ and $\frac{dV_s^*}{dt}$ in simulations or even experiments to precisely limit the inrush current. It lacks generality for different load conditions and additional degree of freedom to optimize the start-up time.

## III. Proposed Closed-Loop Black Start-Up Control

The DAB converter has normally three control variables, which are the inner phase-shift ratios $D_p$ and $D_s$ for the input bridge and the output bridge, respectively, and the outer phase-shift ratio $D_\varphi$ between two bridges, as depicted in Fig. 3. To minimize the start-up time, an operation mode is desired to deliver the maximum output current with a limited transformer peak current under the low-output-voltage condition.

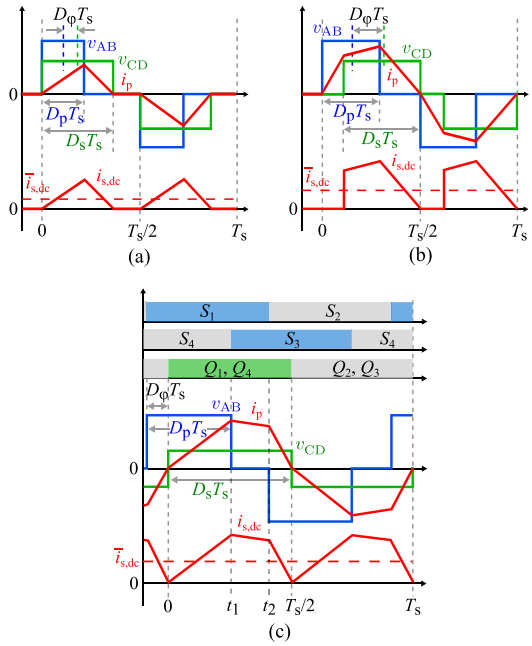


Fig. 3. Switching patterns and waveforms of the selected modulation modes. (a) TPS-TCM ($d < 1$). (b) TPS-TZM. (c) Dedicated EPS-TZM.

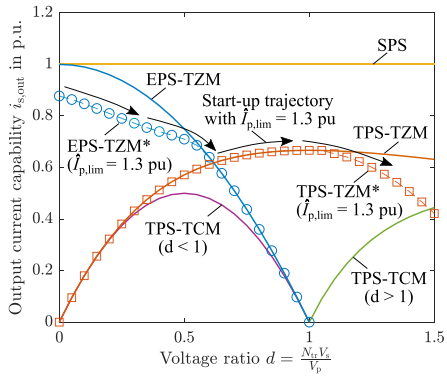


Fig. 4. Output current capability of different modulation schemes.

As already mentioned, the SPS modulation is not suitable for the soft start-up operation due to the large inrush current, although it can deliver the highest possible output current, i.e., $\frac{V_p}{8fL_\sigma} = 1$ p.u. [1], as depicted in Fig. 4. On the other hand, the TPS with the triangular-current modulation (TPS-TCM), as depicted in Fig. 3(a), can limit the inrush current, which is similar to the open-loop ramp phase in the conventional soft start-up method. But the maximum output current of the TPS-TCM mode is limited when the voltage ratio $d = \frac{N_{tr}V_s}{V_p}$ is very low, as shown in Fig. 4. As an extension of the TPS-TCM mode [8], the TPS with the trapezoidal-current modulation (TPS-TZM), as depicted in Fig. 3(b), can further increase the maximum output current, but the difference is only remarkable when $d$ is above 0.4, as depicted in Fig. 4. The analytical expression of the output current for the aforementioned modulation modes can be found in Table I [8].

To fill in the gap in the range of a very low $d$, the extended phase shift with the trapezoidal current modulation (EPS-TZM)

TABLE I
EXPRESSIONS OF THE OUTPUT CURRENT FOR RELATED MODULATION MODES

| Mode | $D_\mathrm{p}$ | $D_\mathrm{s}$ | $I_\mathrm{s,out}$ | $I_\mathrm{s,out,max}$ | $I_\mathrm{s,out,min}$ |
|---|---|---|---|---|---|
| TPS-TCM ($d<1$) | $\frac{2dD_\varphi}{1-d}$ | $\frac{2D_\varphi}{1-d}$ | $\frac{4dV_\mathrm{p}D_\varphi^2}{fL_\sigma(1-d)}$ | $\frac{d(1-d)V_\mathrm{p}}{4fL_\sigma}$ | 0 |
| TPS-TCM ($d>1$) | $\frac{2dD_\varphi}{(d-1)}$ | $\frac{2D_\varphi}{(d-1)}$ | $\frac{4V_\mathrm{p}D_\varphi^2}{fL_\sigma(d-1)}$ | $\frac{(d-1)V_\mathrm{p}}{4fL_\sigma d^2}$ | 0 |
| TPS-TZM | $\frac{d(1-2D_\varphi)}{1+d}$ | $\frac{(1-2D_\varphi)}{1+d}$ | $\frac{V_\mathrm{p}[2d(1-8D_\varphi^2)-(1+d^2)(1-4D_\varphi)^2]}{4fL_\sigma d(1+d)^2}$ | $\frac{dV_\mathrm{p}}{4fL_\sigma(1+d+d^2)}$ | $\frac{d(1-d)V_\mathrm{p}}{4fL_\sigma}$ for $d<1$ or $\frac{(d-1)V_\mathrm{p}}{4fL_\sigma d^2}$ for $d>1$ |
| SPS | 0.5 | 0.5 | $\frac{V_\mathrm{p}D_\varphi(1-2D_\varphi)}{fL_\sigma}$ | $\frac{V_\mathrm{p}}{8fL_\sigma}$ | 0 |
| EPS-TZM | $2D_\varphi+0.5d$ | 0.5 | $\frac{V_\mathrm{p}[-8D_\varphi^2+4(1-d)D_\varphi-d^2+d]}{4fL_\sigma}$ | $\frac{(1-d^2)V_\mathrm{p}}{8fL_\sigma}$ | $\frac{d(1-d)V_\mathrm{p}}{4fL_\sigma}$ |

is proposed for $d<1$, as shown in Fig. 3(c). As another form of extension from the TPS-TCM mode, the EPS-TZM fixes $D_\mathrm{s}=0.5$ to maximize the output current, and adjusts $D_\varphi$ and $D_\mathrm{p}$ to limit the peak current while realizing zero-current switching (ZCS) for the output bridge. The switches in the input bridge can realize zero-voltage switching (ZVS). The transformer current is calculated as

$$i_\mathrm{p}(t)=\begin{cases} i_\mathrm{p}(0)+\frac{(1-d)V_\mathrm{p}t}{L_\sigma} & \text{for } 0\le t\le t_1 \\ i_\mathrm{p}(t_1)-\frac{dV_\mathrm{p}(t-t_1)}{L_\sigma} & \text{for } t_1\le t\le t_2 \\ i_\mathrm{p}(t_2)-\frac{(1+d)V_\mathrm{p}(t-t_2)}{L_\sigma} & \text{for } t_2\le t\le \frac{T_\mathrm{s}}{2} \end{cases} \tag{1}$$

where $t_1=D_\mathrm{p}T_\mathrm{s}-D_\varphi T_\mathrm{s}$ and $t_2=0.5T_\mathrm{s}-D_\varphi T_\mathrm{s}$. $T_\mathrm{s}=\frac{1}{f}$ denotes the switching period, where $f$ is the switching frequency.

Assigning $i_\mathrm{p}(0)=-i_\mathrm{p}(\frac{Ts}{2})=0$ yields

$$D_\mathrm{p}=2D_\varphi+0.5\,d. \tag{2}$$

The transformer peak current is expressed as

$$i_\mathrm{p-pk}=i_\mathrm{p}(t_1)=\frac{(1-d)(2D_\varphi+d)V_\mathrm{p}}{2fL_\sigma}. \tag{3}$$

The output current of the EPS-TZM mode is expressed as

$$i_\mathrm{s,out}=\frac{V_\mathrm{p}[-8D_\varphi^2+4(1-d)D_\varphi-d^2+d]}{4fL_\sigma}. \tag{4}$$

From (4), the maximum and minimum values of the output current are derived

$$\begin{cases} i_\mathrm{s,out,max}=\frac{(1-d^2)V_\mathrm{p}}{8fL_\sigma} \text{ at } D_\varphi=\frac{1-d}{4} \\ i_\mathrm{s,out,min}=\frac{d(1-d)V_\mathrm{p}}{4fL_\sigma} \text{ at } D_\varphi=0. \end{cases} \tag{5}$$

According to (5), $i_\mathrm{s,out,max}$ of the EPS-TZM mode decreases quadratically with an increasing $d$. As depicted in Fig. 4, the EPS-TZM mode can deliver a significantly higher output current than the TPS-TZM mode when $d<0.6$, which fills in the gap under the condition of a very low output voltage.

Thereafter, the maximum allowable precharge current with a limited current stress can be conveniently determined in the following steps.

1) Identify the nominal current stress $\hat{I}_\mathrm{p,nom}$ at the nominal voltage and power rating.
2) Predefine the maximum allowable current stress $\hat{I}_\mathrm{p,lim}\ge\hat{I}_\mathrm{p,nom}$ for the start-up procedure depending on the current rating, safe operating area, and the cooling capacity of the devices. The potential maximum transformer peak current of the EPS-TZM mode can be calculated by (3) with $D_\varphi=\frac{1-d}{4}$. When $i_\mathrm{p-pk}$ needs to be limited to a lower value $\hat{I}_\mathrm{p,lim}$, steps 3) and 4) are conducted.
3) Substitute $\hat{I}_\mathrm{p,lim}$ into (3) to obtain the maximum allowable $D_\mathrm{\varphi,max}$ of the EPS-TZM mode.
4) Substitute $D_\mathrm{\varphi,max}$ into (4) to obtain the maximum allowable precharge current of the EPS-TZM mode. Similar procedure can be applied to determine the maximum allowable precharge/output current of the TPS-TZM mode.

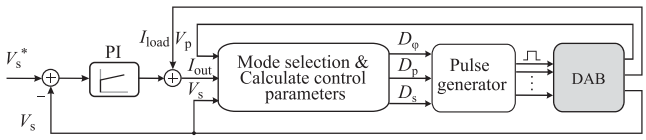


Fig. 5. Generic closed-loop control block diagram of the DAB converter.

As an example, the maximum allowable $i_\mathrm{s,out}$ of the EPS-TZM and TPS-TZM modes for $\hat{I}_\mathrm{p,lim}=1.3$ p.u. are depicted in Fig. 4 (marked with *). Following the upper boundary of these two modes constrained by $I_\mathrm{p,lim}$, the DAB converter can start up from zero to the nominal output voltage with the maximum allowable output current. This cannot only limit the inrush current but also minimize the start-up time. Moreover, due to the ZCS nature of the trapezoidal current, a smooth transition of the transformer current is realized from the EPS-TZM to the TPS-TZM mode with soft-switching operation in the whole start-up procedure.

More importantly, the proposed EPS-TZM mode can be generically implemented in the closed-loop controller together with other modulation modes, such as TPS-TZM and TPS-TCM, as depicted in Fig. 5. A standard voltage PI regulator is adopted to produce the reference output current. With the measured voltage ratio, the maximum allowable output currents of the EPS-TZM, TPS-TCM, and TPS-TZM modes with a limited peak current $\hat{I}_\mathrm{p,lim}$ are then calculated and compared with the reference output current to select the proper mode, as referred to Fig. 4. An antiwindup is required to limit the output reference current and avoid a saturation of the integrator. Due to a large voltage error in the beginning of the black start-up, the reference output current will be instantaneously set to the maximum allowable output current of the EPS-TZM mode. With an increasing $d$, the modulation mode is automatically transited to TPS-TZM or TPS-TCM until the reference output voltage is reached. Benefited from the closed-loop control implementation, the proposed black start-up method is inherently adaptive to different load

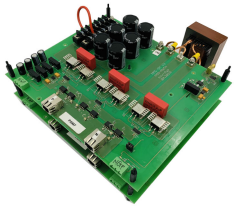

Fig. 6. DAB converter prototype.

TABLE II
EXPERIMENTAL PARAMETERS

| | |
|---|---|
| Input dc voltage | 80 V |
| Output dc voltage reference | 90 V |
| Total leakage inductance | 29 μH |
| Transformer turns ratio | 1:1 |
| Switching frequency | 20 kHz |
| Output capacitance | 2 mF |
| Proportional gain | 1.244 |
| Integral gain | 39.081 |

conditions, which avoids complex process of parameter tuning as in the conventional method.

## IV. EXPERIMENTAL VALIDATION

Experiments are performed on a down-scaled DAB converter prototype (as shown in Fig. 6) to compare the black start-up performance of the conventional and the proposed methods under different load conditions. Detailed parameters of the DAB converter are given in Table II. It is worth mentioning that the potential maximum transformer peak current during the black start-up procedure is $\frac{V_\mathrm{p}}{4fL_\sigma} = 34.5\,\mathrm{A}$ at $V_\mathrm{s} = 0\,\mathrm{V}$ with $D_\mathrm{p} = D_\mathrm{s} = 0$ and $D_\varphi = 0.25$, which is too large for the designed prototype. Notice that the peak current under the nominal voltage and power condition is only about 12 A. Therefore, in the experiments, the maximum transformer peak current is always limited to 15 A, which is approximately 25% higher than the steady-state peak current for a nominal power of 600 W at $V_\mathrm{s} = 90\,\mathrm{V}$.

Fig. 7 depicts the measured black start-up waveforms under the no-load condition. For the conventional soft start-up method, the slope ramp-rates of $D_\mathrm{p}$ and $V_\mathrm{s}^*$ are carefully tuned to $\frac{\mathrm{d}D_\mathrm{p}}{\mathrm{d}t} = 0.022/\mathrm{ms}$ and $\frac{\mathrm{d}V_\mathrm{s}^*}{\mathrm{d}t} = 5\ \mathrm{V/ms}$, respectively, to limit the maximum peak current to 15 A. This results in a start-up period of $t_\mathrm{start} = 37.6\,\mathrm{ms}$ and a maximum peak current of 15.3 A, as shown in Fig. 7(a). When the proposed method is applied, $V_\mathrm{s}$ ramps to the nominal voltage of 90 V within only 21.2 ms, as shown in Fig. 7(b), which is significantly reduced by 43.6% compared to the conventional method. Moreover, the transformer peak current in the proposed method is not only limited to 15 A but also maintained close to the maximum allowable peak current during the whole start-up procedure, which is distinguished from the conventional method.

Fig. 8 depicts the measured black start-up waveforms when a load resistor $R_\mathrm{load} = 13.5\,\Omega$ ($P_\mathrm{nom} = 600\,\mathrm{W}$) is connected. For the conventional method, the slope ramp-rates are retuned to $\frac{\mathrm{d}D_\mathrm{p}}{\mathrm{d}t} = 0.0125/\mathrm{ms}$ and $\frac{\mathrm{d}V_\mathrm{s}^*}{\mathrm{d}t} = 0.8\ \mathrm{V/ms}$ for the same

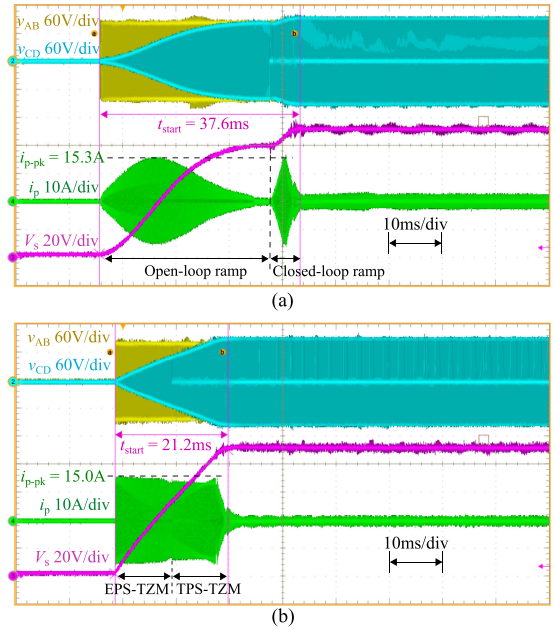


Fig. 7. Measured black start-up waveforms under the no-load condition with a maximum transformer peak current of 15 A. (a) Conventional method. (b) Proposed method.

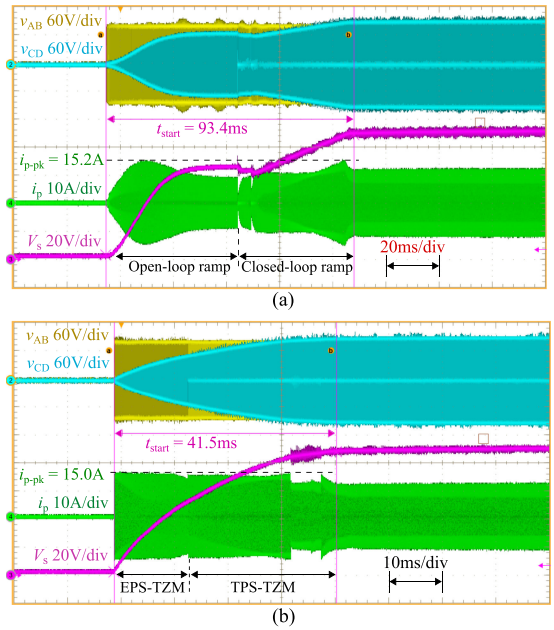


Fig. 8. Measured black start-up waveforms with a load resistor $R_\mathrm{load} = 13.5\,\Omega$ (600 W at $V_\mathrm{s} = 90\,\mathrm{V}$) and a maximum transformer peak current of 15 A. (a) Conventional method. (b) Proposed method.

maximum peak current, which result in a start-up period of $t_\mathrm{start} = 93.4\,\mathrm{ms}$, as shown in Fig. 8(a). It can be noticed that the slope-rate of $V_\mathrm{s}$ becomes very low in the end of the open-loop ramp stage due to a relatively large load current. Therefore, to minimize the start-up time, the closed-loop ramp stage has already started when $V_\mathrm{s} \geq 64\,\mathrm{V}$, i.e., $0.8V_\mathrm{p}$. On the other hand, when the proposed method is applied, the start-up period is 41.5 ms with even a 55.6% reduction, as shown in Fig. 8(b).

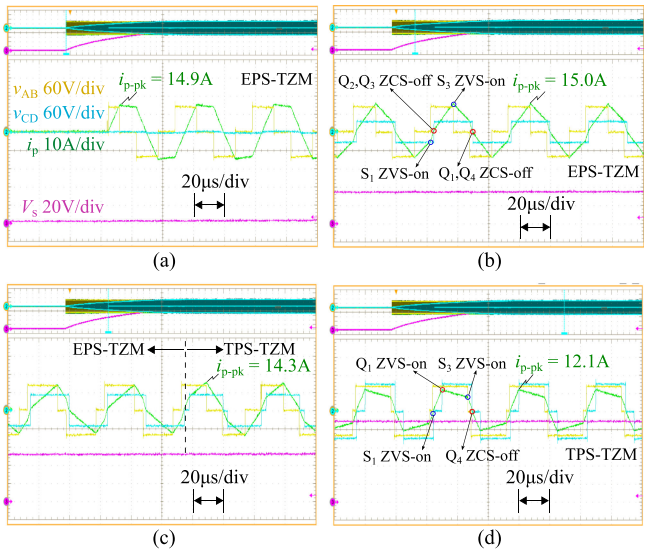


Fig. 9. Zoomed-in waveforms of the proposed black start-up control with $R_{\text{load}} = 13.5\,\Omega$ in Fig. 8(b). (a) Initial EPS-TZM waveforms at $V_{\text{s}} = 0$ V. (b) EPS-TZM mode at $V_{\text{s}} = 35$ V. (c) Mode transition from EPS-TZM to TPS-TZM at $V_{\text{s}} = 52$ V. (d) TPS-TZM mode at $V_{\text{s}} = 90$ V.

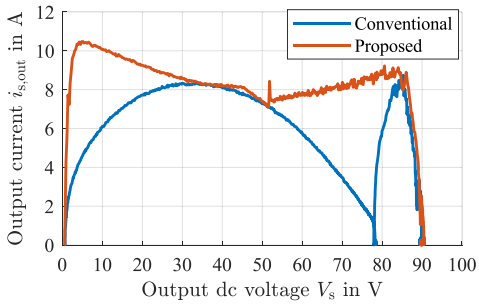


Fig. 10. Measured no-load start-up trajectories ($i_{\text{s,out}}$ against $V_{\text{s}}$) of the DAB converter with the conventional and the proposed method.

Furthermore, Fig. 9 shows zoomed-in waveforms of the proposed method with $R_{\text{load}} = 13.5\,\Omega$. In Fig. 9(a), the DAB converter starts up in the EPS-TZM mode with $i_{\text{p-pk}} = 14.9$ A at $V_{\text{s}} = 0$ V. In Fig. 9(b), the DAB converter continues to operate in the EPS-TZM mode with the maximum allowable peak current. The ZVS and ZCS are realized for the input and output bridges, respectively. In Fig. 9(c), when $V_{\text{s}}$ increases to 52 V, a mode transition occurs from the EPS-TZM to the TPS-TZM mode with a smooth transformer current. The DAB converter continues to operate in the TPS-TZM mode until reaching the steady state at $V_{\text{s}} = 90$ V, as shown in Fig. 9(d). Enabled by the combination of the EPS-TZM and TPS-TZM modes, the DAB converter realizes ZVS and ZCS operation during the whole start-up procedure.

Fig. 10 shows a comparison of the measured start-up trajectory, i.e., $i_{\text{s,out}}$ against $V_{\text{s}}$, under the no-load condition between the conventional and the proposed methods. It is validated that a higher output current is delivered by the proposed method at almost every value of the output dc voltage.

## V. Conclusion

This letter introduces a novel black start-up control of the DAB converter, which can be generically implemented into the closed-loop controller without complex tuning process. The proposed control is enabled by the EPS-TZM mode, which is able to deliver a high output current with a limited peak value at a very low voltage ratio. Combining the EPS-TZM and TPS-TZM mode, the DAB converter can start up with the maximum allowable output current while maintaining soft-switching operation during the whole start-up procedure. Experiments validate the effectiveness of the proposed method, and demonstrate a significant reduction of the start-up time up to $55.6\%$ compared to the state-of-the-art method.

## References

[1] R. W. A. A. De Doncker, D. M. Divan, and M. H. Kheraluwala, "A three-phase soft-switched high-power-density dc/dc converter for high-power applications," *IEEE Trans. Ind. Appl.*, vol. 27, no. 1, pp. 63–73, Jan. 1991.

[2] J. Hu, "Modulation and dynamic control of intelligent dual-active-bridge converter based substations for flexible dc grids," Ph.D. dissertation, E.ON Energy Res. Center, RWTH Aachen Univ., Aachen, Germany, 2019.

[3] H. Bai and C. Mi, "Eliminate reactive power and increase system efficiency of isolated bidirectional dual-active-bridge dc-dc converters using novel dual-phase-shift control," *IEEE Trans. Power Electron.*, vol. 23, no. 6, pp. 2905–2914, Nov. 2008.

[4] X. Liu, H. Li, and Z. Wang, "A start-up scheme for a three-stage solid-state transformer with minimized transformer current response," *IEEE Trans. Power Electron.*, vol. 27, no. 12, pp. 4832–4836, Dec. 2012.

[5] S. Pugliese, G. Buticchi, R. A. Mastromauro, M. Andresen, M. Liserre, and S. Stasi, "Soft-start procedure for a three-stage smart transformer based on dual-active bridge and cascaded H-bridge converters," *IEEE Trans. Power Electron.*, vol. 35, no. 10, pp. 11 039–11052, Oct. 2020.

[6] Y. Gao, V. Sankaranarayanan, R. W. Erickson, and D. Maksimovic, "Soft startup strategies for DAB-based DCX in composite converters," in *Proc. IEEE Energy Convers. Congr. Expo.*, 2020, pp. 6130–6135.

[7] P. Yao, X. Jiang, and F. F. Wang, "Soft starting strategy of cascaded dual active bridge converter for high power isolated dc-dc conversion," in *Proc. IEEE Appl. Power Electron. Conf. Expo.*, 2020, pp. 1031–1037.

[8] F. Krismer and J. W. Kolar, "Accurate small-signal model for the digital control of an automotive bidirectional dual active bridge," *IEEE Trans. Power Electron.*, vol. 24, no. 12, pp. 2756–2768, Dec. 2009.